



Rapid and sensitive detection of rotavirus by surface-enhanced Raman scattering immunochromatography

Yuxue Zhang^{1,2} · Gang Wu^{1,2} · Jiata Wei^{1,2} · Yanlei Ding² · Yingming Wei¹ · Qiqi Liu² · Hailan Chen¹

Received: 16 September 2020 / Accepted: 24 November 2020 / Published online: 2 January 2021
© Springer-Verlag GmbH Austria, part of Springer Nature 2021

Abstract

A surface-enhanced Raman scattering (SERS) immunochromatographic assay (ICA) has been developed for rapid, ultrasensitive, and quantitative detection of rotavirus in feces using double Raman molecule-labeled Au-core Ag-shell nanoparticles. The Raman signals are generated by 5,5'-dithiobis-(2-nitrobenzoic acid) and the intensity of the characteristic peak at 1334^{-1} cm was detected as the analytical signal. The Raman signals were enhanced by the SERS-enhanced effect of both Au and Ag, the large amount of Raman molecules, and the hot-spot effect in the narrow gap between the Au core and Ag shell. The SERS ICA can quantitatively detect rotavirus in a concentration range of 8–40,000 pg/mL, with detection limits of 80 pg/mL and 8 pg/mL based on naked eye observation and SERS signal detection, respectively. No cross-reaction was observed from other common pathogens. The standard deviation of the intra- and inter-batch repetitive tests is less than 10%, and the coincidence between SERS ICA and RT-qPCR as well as commercial colloidal gold ICA is 100%. The results indicated that this SERS ICA is able to quantitatively detect rotavirus in feces in 20 min with high sensitivity, selectivity, reproducibility, and accuracy and might be a promising method for the early detection of rotavirus in clinical analysis.

Keywords Surface-enhanced Raman scattering · Immunochromatography · Au-core Ag-shell nanoparticles · Rotavirus

Introduction

Rotavirus diarrhea is considered one of the four common diseases in infants and young children, accounting for more than 450,000 children death per year according to the estimation of the World Health Organization (WHO) [1]. Nowadays, rotavirus is still responsible for 37.5% of gastroenteritis cases and 145,000 deaths in developing countries in Asia every year [2, 3]. Rotavirus diarrhea exhibits similar clinical symptoms to infectious gastroenteritis, epidemic diarrhea, *Salmonella* diarrhea, and *Escherichia coli* (*E. coli*) diarrhea; thus, early diagnosis of the etiology can provide guidance for the timely

treatment of acute diarrhea [4]. Available methods for rotavirus detection included morphologic observation, immunological methods detecting rotavirus-specific immunoglobulins or antigen, and molecular biological methods directly detecting antigen [5]. Electron microscopic observation is a classical method for rotavirus detection, but it requires very expensive equipment [6]. Reverse transcription polymerase chain reaction (RT-PCR), quantitative real-time PCR (qPCR), gene-chip technology, and DNA sequencing, targeting the conserved nucleotide sequence of rotavirus, have been widely used in pathogen detection which have high selectivity and sensitivity [7]. However, their wide applications in primary medical institutions and field tests are limited by the requirement of expensive equipment (RT-qPCR and DNA sequencing), expensive reagent (DNA sequencing), or highly skilled performers (PCR) [8]. Serological analysis is a high-throughput method that is easy to perform, but the common false negative result may delay the disease treatment due to the lag in antibody production [9]. Immunological methods directly targeting the antigen of rotavirus, such as enzyme-linked immunosorbent assays (ELISA), have been used in rotavirus detection, but their use was limited by its low sensitivity and requirement of specific machines [10].

Yuxue Zhang and Gang Wu contributed equally to this work.

✉ Qiqi Liu
liuqiqi@bmi.ac.cn

✉ Hailan Chen
hlchen319@163.com

¹ College of Animal Science and Technology, Guangxi University, Nanning 530004, China

² Beijing Institute of Radiation Medicine, Beijing 100850, People's Republic of China

Owing to its advantages of simplicity, fastness, and low cost, immunochromatography assay (ICA) has been considered the most successful point-of-care technique [11]. Currently, ICA has been widely used for the rapid detection of virus, bacteria, disease markers, drug residues, and environmental pollutants [12]. However, the low signal intensity of the color formation reaction based on the accumulation of small-sized Au nanoparticles (NPs) limits the applications of conventional ICA [13]. In addition, most conventional ICAs can only perform qualitative or semi-quantitative detection, which cannot meet the quantitative analysis in certain situations [11, 14]. In recent years, efforts are focusing on increasing the detection sensitivity of ICA and realizing quantitative analysis using new types of labels, such as fluorescence dyes, quantum dots, and magnetic beads [15].

Surface-enhanced Raman scattering (SERS), a phenomenon that Raman signals can be amplified by 10^6 – 10^{14} orders of magnitude when Raman reporters are placed on the surface of colloidal particles or rough surfaces of Au, Ag, Cu, and other metals, provides a new technique for the detection of target molecules in extremely low concentrations [16, 17]. SERS-encoded particles (or SERS tags), prepared by conjugating Raman reporter molecules to the plasmonic metal nanoparticles, have been considered a new class of labeling agents. In recent years, SERS is introduced into the ICA system to develop the new detection system of SERS ICA [18, 19]. Au nanoparticles (AuNP) [20], hollow AuNP [21], Au@Ag core-shell NPs [22], Au nanostar@Raman reporter@silica sandwich nanoparticles [23], and other kinds of nanoparticles have been used as a signal generation element in SERS ICA. Compared to the traditional gold colloidal ICA, two to three orders of improvements at the limit of detection have been reported from these new ICA systems. In addition to the available numerous affordable handheld Raman spectrometers in the market today, SERS ICA is a promising POCT technique with the advantages of ultra-sensitivity, time-saving, and qualitative detection and has been applied in the selectivity and sensitive detection of viral nuclei acid, cancer markers, bacteria, heavy metal chromium, etc. [24].

Herein, we developed a SERS ICA for the rapid, sensitive, and quantitative detection of rotavirus in feces for the first time. To develop this SERS ICA, rotavirus-specific SERS tags were prepared by immobilizing mouse anti-rotavirus monoclonal antibody to the double-layer Raman molecule-labeled Au-core Ag-shell nanoparticle. After ICA procedures, the color and specific Raman scattering intensity at 1334 cm^{-1} of Raman molecule on the test line were observed and measured for the qualitative and quantitative detection of rotavirus. The analytical results on clinical sample detection were compared with an established real-time quantitative PCR (RT-qPCR) and commercial colloidal gold ICA. The proposed SERS ICA displayed the properties of high sensitivity, selectivity, accuracy, and precision for rotavirus detection.

Experimental section

Materials

Nitrocellulose (NC) membrane, conjugate pad, sample pad, absorbent pad, and polyvinyl chloride (PVC) bottom plate were purchased from Shanghai Jieyi Biotechnology, China. Tetrachloroauric acid (HAuCl_4), silver nitrate (AgNO_3), sodium citrate, 5,5'-dithiobis-(2-nitrobenzoic acid) (DTNB), 1-(3-dimethylaminopropyl)-3-ethylcarbodiimide hydrochloride (EDC), N-hydroxysuccinimide (NHS), and bovine serum albumin (BSA) were bought from Sigma, USA. Polyvinyl pyrrolidone (PVP), sucrose, and Tween-20 were obtained from Sinopharm Chemical Reagent Co., Ltd., China. Mouse anti-rotavirus monoclonal antibodies (Ab_1 and Ab_2) were bought from US-China Xinxin Biotechnology Co., Ltd., China. The rotavirus reference materials for ICA were purchased from the China Institute of Food and Drug Control. Colloidal gold ICA test strips were purchased from Guangzhou Wanfu Biotechnology Co., Ltd.

Instruments

A Hitachi H-9000 transmission electron microscopy (TEM) and a Tecnai G2 F20 TEM (FET, USA) were used for the morphological characterization of NPs. A Genesis Energy Spectrometer was employed for the element analysis of the nanoparticles (EDAX, USA). UV-Vis spectra were acquired by scanning between the wavelengths of 190 and approximately 800 nm on a Shimadzu 2600 spectrometer. Raman spectra were recorded on an i-Raman Plus B WS465-785H spectrometer (B&W TeK, USA) coupling with a BX51 optical microscope (Olympus, Japan). The excitation laser is 785 nm and then focused to a 2-mm-diameter spot via a $\times 5$ objective during Raman signal detection. For Raman signal detection, the acquisition time was set as 5 s and the excitation power was set as 5%. The signal intensities were normalized according to the silicon wafer at 520 cm^{-1} .

Synthesis and characterization of Au/DTNB@Ag/DTNB nanoparticles

Double-layer DTNB-labeled Au-core Ag-shell nanoparticles (Au/DNTB@Ag/DTNB NPs) were synthesized according to a previous report and the detailed procedure can be found in the supporting information [25]. The morphologies of Au nanoparticles (Au NPs), Au/DTNB NPs, and Au/DNTB@Ag/DTNB NPs were observed with TEM. The UV spectra and Raman spectra were recorded to evaluate their optical characteristics.

Fabrication of rotavirus-specific SERS tags

A total of 20 mL Au/DTNB@Ag/DTNB NP solution was centrifuged at 8000 rcf for 15 min. The supernatant was carefully removed and the precipitate was resuspended in 1 mL deionized water. The carboxyl groups of DTNB were activated by 50 μ M EDC and NHS at RT for 15 min on an oscillometer. Excess EDC and NHS were removed by centrifuging at 7000 rcf for 7 min and the precipitate was resuspended in 500 μ L borate buffer (BB, 2 mM, pH 8.0). Mouse anti-rotavirus monoclonal antibody 1 (Anti-RV mAb1, 25 μ g) was conjugated to Au/DTNB@Ag/DTNB NPs by shaking at RT for 2 h. The remaining active sites were blocked with BSA (10%, w/v, 100 μ L) for another 1 h. The mixture was then centrifuged at 7000 rcf for 7 min and the precipitate was washed with BB (2 mM, pH 8.0) 4 times. The obtained product, denoted as rotavirus-specific SERS tags, was finally resuspended with 500 μ L preservation solution and stored at 4 °C for further use. The preservation solution is Tris-HCl buffer (50 mM, pH 8.0) containing 1% BSA (w/v), 0.1% PVP (w/v), 10% sucrose (w/v), and 0.5% Tween-20 (v/v).

Assembling of SERS ICA strips

Mouse anti-rotavirus monoclonal antibody 2 (Anti-RV mAb2, 0.5 mg/mL) and goat anti-mouse IgG (0.5 mg/mL) were sprayed on the NC membrane using a Biodot xyz5050 to prepare the test line (T line) and control line (C line), respectively. The membrane was dried at 37 °C for 3 h to allow the antibodies to firmly fix on the NC membrane. Rotavirus-specific SERS tags were sprayed on the conjugate pad and dried at 37 °C for 3 h. The sample pad, prepared conjugate pad, coated NC membrane, and absorbent pad were then affixed on a PVC bottom plate in sequence and cut into strips with 3 mm width. The prepared SERS ICA strips were kept at dry and dark conditions for further use.

Detection of rotavirus using SERS ICA strips

To detect rotavirus, rotavirus standard samples were diluted with phosphoric buffer saline (PBS, 10 mM, pH 7.4) supplemented with 0.05% Tween-20 (PBST) and 60 μ L was dropped on the sample pad of prepared SERS ICA strips. The visualization results were observed and imaged after keeping at RT for 10 min, while the Raman spectra at the T line area were recorded on a Raman spectrometer in 20 min. A total of ten points were randomly selected from left to right at distance of 50 μ m at the T line area of each strip. The average Raman intensity at 1334 cm^{-1} was calculated for each strip.

The sensitivity of SERS ICA strips

To analyze the sensitivity of the SERS ICA strips, positive rotavirus standard samples with an original concentration of 4000 ng/mL (purchased from the China Institute of Food and Drug Control) were series diluted with PBST to final concentrations of 40,000 pg/mL, 8000 pg/mL, 4000 pg/mL, 800 pg/mL, 400 pg/mL, 80 pg/mL, 40 pg/mL, 8 pg/mL, and 4 pg/mL. The detection limit based on visual observation was determined as the lowest concentration with observable T lines using the naked eyes. The limit of detection (LOD) based on the Raman signal was determined as the concentration corresponding to the average Raman intensity at 1334 cm^{-1} of three negative samples plus 3 times of its standard deviation (Raman intensity of LOD = average Raman intensity of negative samples + $3\delta_{\text{negative}}$, where δ is the standard deviation of the Raman intensity of three negative samples). A fitting curve between the Raman intensity of T line and the concentration of rotavirus was also plotted using the Origin 8.0 for the quantitative detection of rotavirus.

The selectivity of SERS ICA strips

The selectivity of the SERS ICA strips was analyzed using 5 rotavirus-positive standard samples and 9 other pathogen-positive standard samples obtained from the China Institute of Food and Drug Control. The rotavirus-positive standard samples include G2 subtype rotavirus-positive standard (P1), G3 subtype rotavirus-positive standard (P2), G4 subtype rotavirus-positive standard (P3), G8 subtype rotavirus-positive standard (P4), and G9 subtype rotavirus-positive standard (P5). Other pathogen-positive standard samples include Coxsackievirus type A16 (N1), enteric adenovirus type 71 (N2), norovirus (N3), adenovirus (N4), *Escherichia coli* (N5), *Salmonella* paratyphoid A (N6), *Salmonella* paratyphi B (N7), *Salmonella* paratyphi C (N8), *Yersinia enterocolitica* (N9), and *Staphylococcus aureus* (N10).

Repeatability analysis of SERS ICA strips

Ten strips randomly selected from the same batches of rotavirus SERS ICA strips and another 8 strips selected from 8 different batches were used to detect the same diluted rotavirus standard samples for the determination of its in-run repeatability and between-run repeatability, respectively. Raman signal intensity of the main peak at 1334 cm^{-1} was used to calculate the coefficient of variation according to the formula of CV = standard deviation (SD)/mean \times 100%.

Detection of clinical samples

In order to verify the validity of the SERS ICA strips, 95 clinical feces samples preserved by the Beijing Institute of

Radiation Medicine were tested by SERS ICA, RT-qPCR, and colloidal gold ICA. Results obtained from these methods were compared to determine the validity of the SERS ICA strips. The primers and probes for the RT-qPCR are shown in Table 1.

To detect clinical samples, a sterile tube was used to collect the feces samples. Two grams of the solid stool specimens or 100 μL of liquid sample was homogenized in 1 mL of PBST. After standing for 10 min at room temperature, 60 μL of the supernatant was dropped on the sample pad of prepared SERS ICA strips and results were determined as in the section “Detection of rotavirus using SERS ICA strips.”

Results and discussion

Principle of SERS ICA

The principle of rotavirus detection based on SERS ICA is similar to that of a previous work finished in our lab and shown in Fig. 1 [25]. Firstly, a double-layer Raman molecule (DTNB)-labeled Au-core Ag-shell NP (Au/DTNB@Ag/DTNB NP) is synthesized and conjugated with anti-RV mAb1 to prepare rotavirus-specific SERS tags (Fig. 1a). The SERS ICA strip is composed of sample pad, conjugate pad, NC membrane, and absorbent pad (Fig. 1b). The prepared rotavirus-specific SERS tags are sprayed on the conjugate pad, while the NC membrane is coated with anti-RV mAb2 and goat anti-mouse IgG as T and C lines, respectively. When a positive sample is dropped on the sample pad, the solution flows through the conjugate pad and NC membrane under the capillary action. The SERS tags on the conjugate pad specifically recognize rotavirus in the sample and form rotavirus-SERS tag complexes. The complexes are captured by anti-RV mAb2 coated on the NC membrane to form the antibody-rotavirus-SERS tag complexes when they pass through the T line. As the complexes accumulate, a red line is visualized at the T line area, which also give out Raman signals when they are detected by a Raman spectrometer. The remaining rotavirus-SERS tag complexes and free SERS tags are captured by the goat anti-mouse IgG when they pass through the C line area to present another visualized red line with Raman

signals. When there is no rotavirus in the sample, the SERS tags directly pass through the T line and are captured by the antibody coated on the C line area, showing only one red line. The SERS signal of the T line is used to calculate the concentration of rotavirus based on the standard curve to realize quantitative detection of rotavirus.

Preparation and characterization of SERS tags

In this study, double-layer Raman molecule-labeled Au-core Ag-shell NPs (Au/DTNB@Ag/DTNB NPs) were prepared as the SERS NPs. From Fig. 2, the colloidal Au NPs obtained by citrate reduction method exhibit a sphere shape with a diameter of ~ 25 nm, and their size increased to ~ 40 nm after covering with the Ag shell. From the HR-TEM (inset in Fig. 2b), the thickness of the Ag shell is around 5 nm. The EDS results show that, except common elements of C, N, and O, only Au element is present on the Au NP samples (Fig. 2c). After the coating of the Ag layer, both Ag and Au are detected from the sample of Au/DTNB@Ag/DTNB NPs (Fig. 2d). The S element detected from the Au/DTNB@Ag/DTNB sample might be contributed by the double-layer DTNB molecules which have double -SH groups in their molecular structure.

The color of the colloidal Au NP changed from red violet to orange, indicating the formation of Ag shell on the surface of Au NPs (Fig. 3a). From Fig. 3b, Au NPs, Au/DTNB NPs, Au/DTNB@Ag NPs, and Au/DTNB@Ag/DTNB NPs showed similar shapes in their UV spectra, but the coating of Au core with Ag shell induced a blue shift of 18 nm on the main absorption peaks at ~ 525 nm. In addition, the peak width of NPs with Ag shell covering is narrower than that of Au NP and Au/DTNB NP, suggesting that the synthesis of Ag shell on the Au NP makes the NPs more uniform. Characteristic signals were obtained from the DTNB molecules on the surface of Au NP. From Fig. 3c, no characteristic Raman peaks were observed from the Raman spectrum of Au NP before coating with DTNB, while 8 characteristic Raman peaks belonging to the Raman molecule of DTNB were clearly observed. SERS signal was further enhanced by covering the Au core with a layer of Ag shell and loading with double layers of DTNB molecules.

Table 1 Primer and probe sequence for RT-qPCR

Primer/probe	Sequence
F1	5'-GGCTTTAAAAGCGAGAATTTCCG-3'
R1	5'-AGAATTGTGGTATATTCAATACCATACAT-3'
P	FAM-AAAGGAGCTAACCGTAGCCAGACGG-BHQ1
F2	5'-ACCATCTWCACRTRCCCTC-3'
R2	5'-GGTCACATAACGCCCTATA-3'
P	FAM-ATGAGACAATAGT/iBHQ1dT/AAAAGCTAACACTGTCAA-P

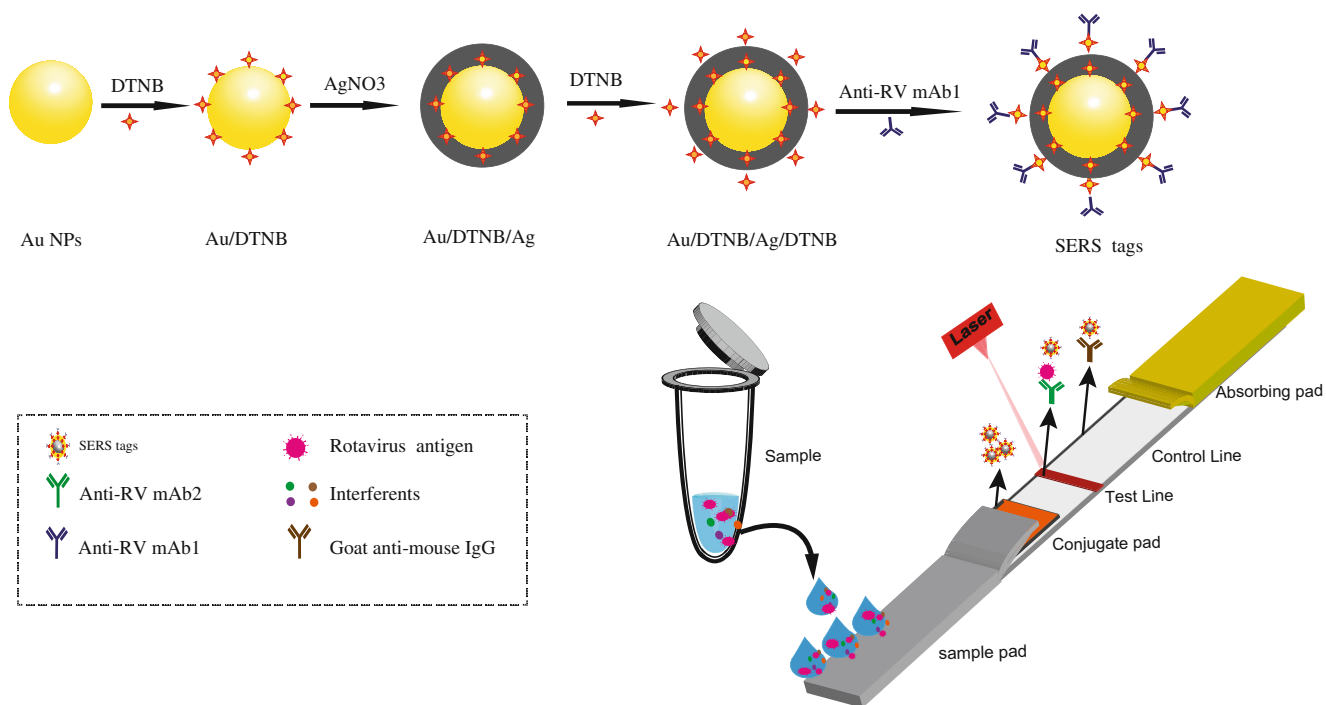


Fig. 1 Schematic of SERS ICA based on double-layer Raman molecule-labeled Au-core Ag-shell (Au/DTNB@Ag/DTNB) nanoparticles. **a** Schematic of the preparation of Au/DTNB@Ag/DTNB SERS tags. **b** Schematic of SERS ICA strip for rotavirus detection

To increase the sensitivity of the SERS ICA, it will be desirable to use NPs with strong Raman signals to label the

detection antibody. Compared with other noble metals, the SERS-enhanced capability of Ag is much stronger, and

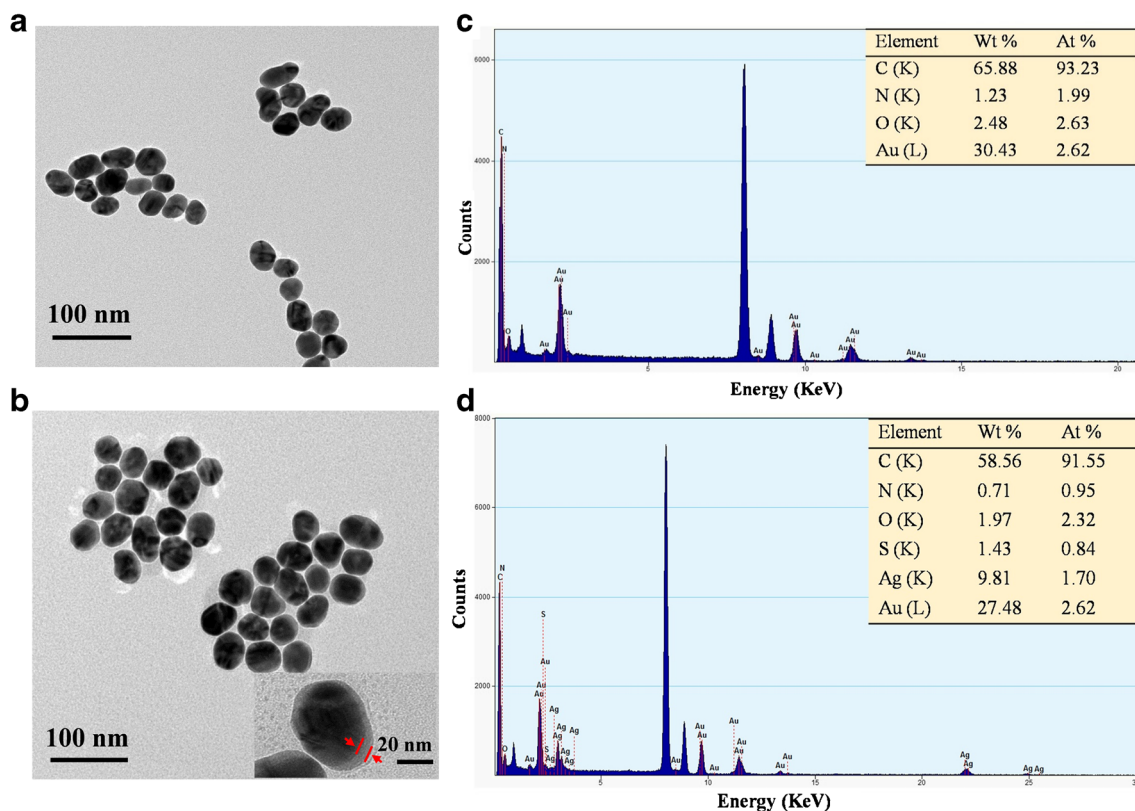


Fig. 2 Surface and element characterization of SERS NPs. **a** TEM images of Au NPs. **b** TEM images of Au/DTNB NPs and Au/DTNB@Ag/DTNB NPs, inset is the high-resolution TEM images of Au/DTNB@Ag/DTNB NPs. **c**, **d** EDS result of Au NPs and Au/DTNB@Ag/DTNB NPs

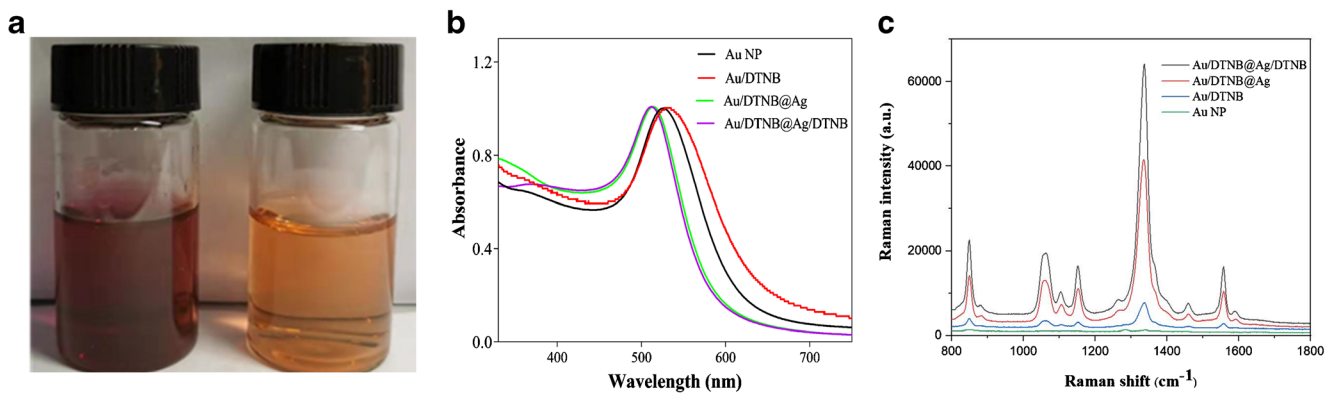


Fig. 3 Optical characterization of SERS NPs. **a** Photos of Au NP solution and Au/DTNB@Ag/DTNB NPs. **b** The UV spectra of Au NPs, Au/DTNB NPs, Au/DTNB@Ag NPs, and Au/DTNB@Ag/DTNB NPs. **c**

SERS spectra of Au NPs, Au/DTNB NPs, Au/DTNB@Ag NPs, and Au/DTNB@Ag/DTNB NPs

10~100 times stronger SERS-enhanced performance has been reported from Ag NPs compared with that from Au NPs [26]. However, it is difficult to prepare Ag NPs with high biocompatibility, narrow size distribution, and good stability. Favoring the advantages of easy preparation, homogeneity, and biocompatibility with biomolecules, Au NPs were used as the core for the synthesis of SERS substrate in this study. In this study, the synthesis of Ag shell on the Au core significantly enhances the Raman signals, especially the main peak at 1334 cm^{-1} . The coating of the second layer DTNB molecules on the surface of the Ag shell further increased the Raman signal, and the Raman intensity of the main peak is almost 10 times higher than that of Au/DTNB NP. It has been reported that the coupling effect of the two surfaces on Au core and Ag shell contributes to the strong SERS signals of the Raman molecules standing in the interior gap between Au core and Ag shell [27]. In this study, the second layer of DTNB molecules provides a larger number of Raman molecules on each NP, which further enhances the SERS signal

under the same target concentration. In sum, there might be three reasons accounting for the strong Raman signals observed on Au/DTNB@Ag/DTNB, including the SERS-enhanced effect of both Au and Ag NP, a large amount of DTNB molecules, and the hot-spot effect in the narrow gap between the Au core and Ag shell.

Sensitivity of SERS ICA strips

Series diluted rotavirus-positive standard samples were detected to evaluate the sensitivity of the rotavirus SERS ICA strips. From Fig. 4a, the color of T line became lighter as the decrease of rotavirus concentration, and the lowest detectable concentration is 80 pg/mL based on naked eye observation. The Raman signal intensity increased as the rotavirus concentration increases, especially the peak at 1334 cm^{-1} which is still visible when the concentration of rotavirus is as low as 8 pg/mL (Fig. 4b). Based on the Raman intensity, the minimum detection limit of the SERS ICA strip is 8 pg/mL which is 10

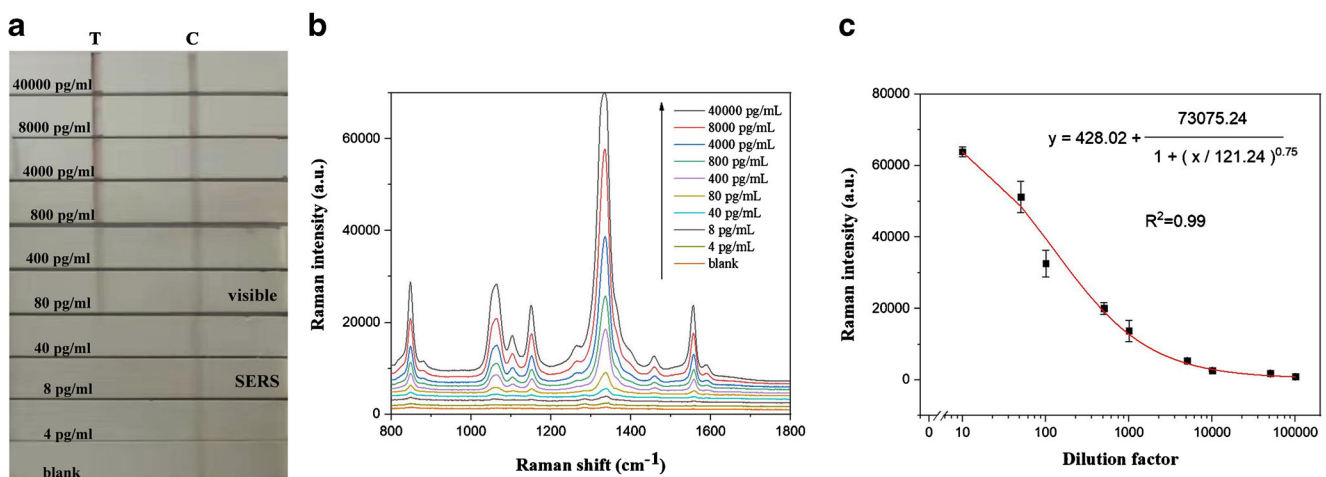


Fig. 4 Detection of series diluted rotavirus-positive standard samples using the SERS ICA strips. **a** Images of SERS ICA strips loaded with series diluted rotavirus standard samples. **b** SERS spectra of the T line

region of corresponding SERS ICA strips. **c** Fitting curve of the Raman signal intensity at 1334 cm^{-1} recorded from the T line area of corresponding SERS ICA strips and rotavirus concentration ($n = 6$)

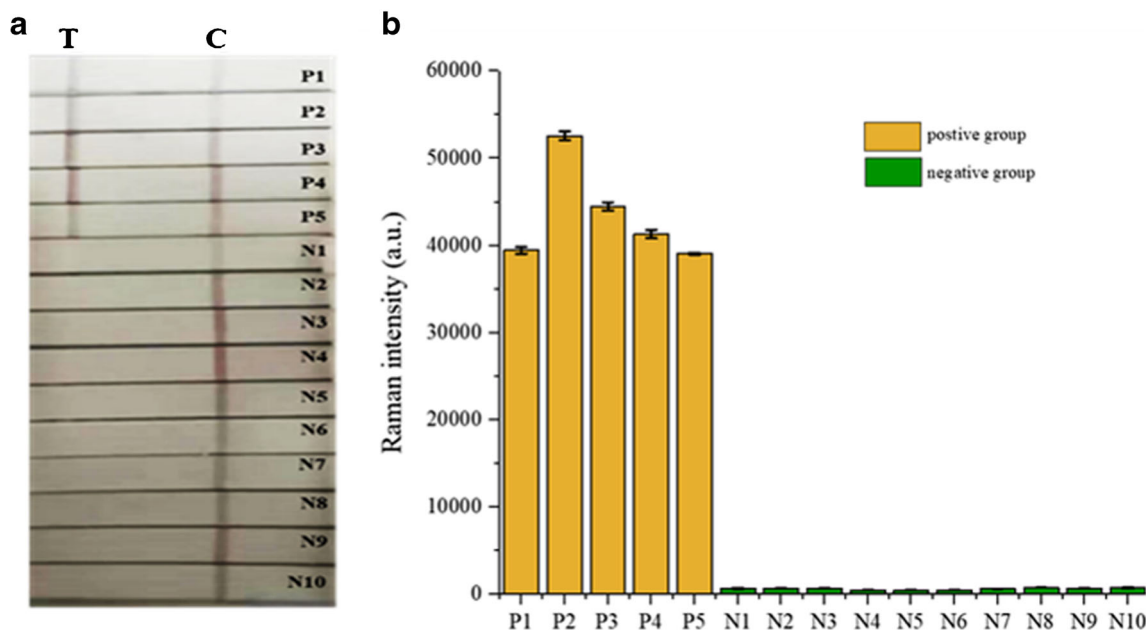


Fig. 5 Determination of the selectivity of rotavirus SERS ICA strips. **a** Images of SERS ICA strips detecting 5 samples positive in different subtypes of rotavirus and 10 samples negative in rotavirus but positive in Coxsackievirus type A16 (N1), enteric adenovirus type 71 (N2), norovirus (N3), adenovirus (N4), *Escherichia coli* (N5), *Salmonella*

paratyphoid A (N6), *Salmonella paratyphi* B (N7), *Salmonella paratyphi* C (N8), *Yersinia enterocolitica* (N9), and *Staphylococcus aureus* (N10). **b** SERS intensity at 1334 cm⁻¹ of the T line region of the corresponding SERS ICA strips (n = 6)

times lower than that based on naked eye observation. A good linear relationship between the SERS signal at 1334 cm⁻¹ and the concentration of rotavirus was obtained with a linear equation of $y = 428.02 + 73,075.24/[1 + (x/121.24)^{0.75}]$ ($R^2 = 0.99$), based on which the quantitative detection of rotavirus can be realized (Fig. 4c).

Selectivity of SERS ICA strips

Five different subtypes of rotavirus standard samples and 10 other kinds of pathogen standards were detected by the SERS

ICA strips to determine its selectivity. Figure 5a shows that obvious T line was observed from the SERS ICA strips loading with G2 subtype rotavirus-positive standard (P1), G3 subtype rotavirus-positive standard (P2), G4 subtype rotavirus-positive standard (P3), G8 subtype rotavirus-positive standard (P4), and G9 subtype rotavirus-positive standard (P5). Strong SERS signal (> 40,000 a.u.) was recorded from the T line region of these SERS ICA strips. However, when Coxsackievirus type A16 (N1), enteric adenovirus type 71 (N2), norovirus (N3), adenovirus (N4), *Escherichia coli* (N5), *Salmonella paratyphoid* A (N6), *Salmonella paratyphi*

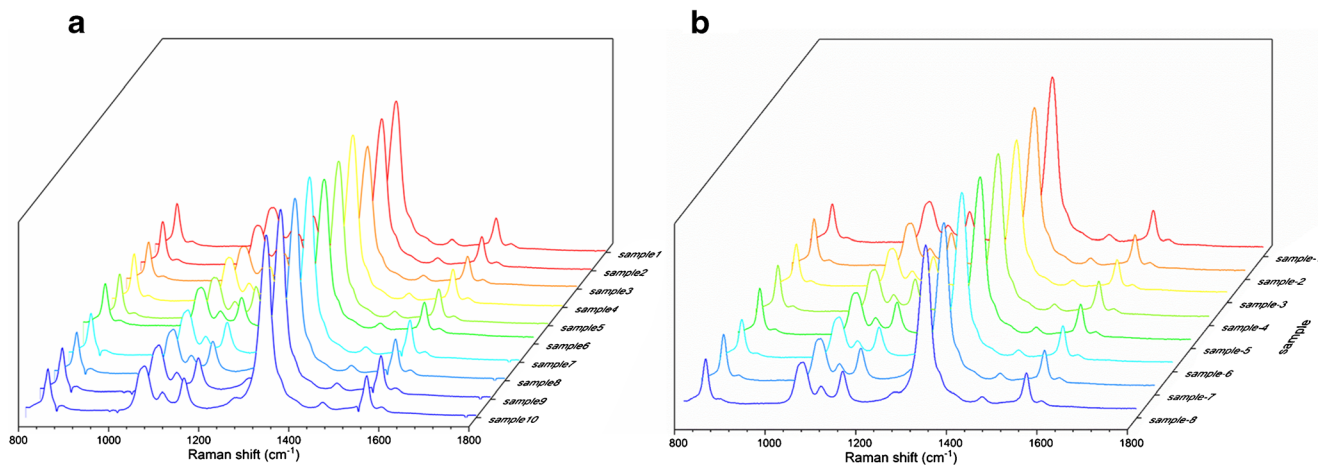


Fig. 6 Raman spectra for the repeatability test using SERS ICA strips. **a** Intra-assay repeatability test using 10 different test strips in the same batch of SERS ICA strips. **b** Inter-assay repeatability test using 8 test strips randomly selected from 8 different batches of SERS ICA strips

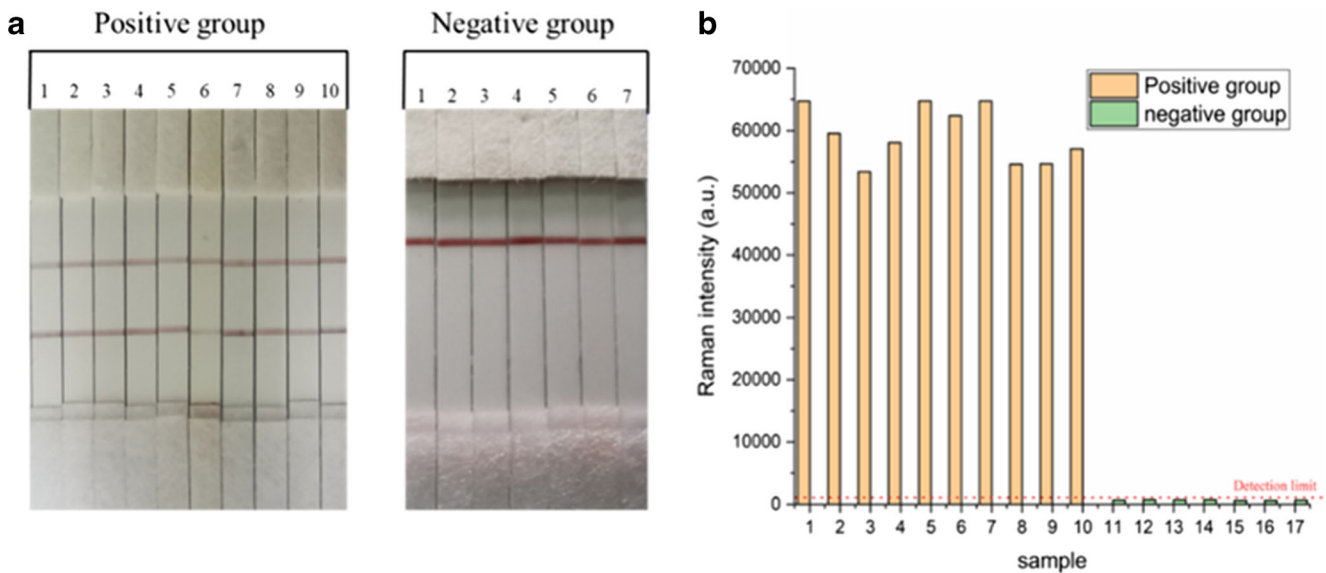


Fig. 7 Determination of the validity of the SERS ICA strips using 95 clinical samples. **a** Images of SERS ICA strips detecting rotavirus-positive and rotavirus-negative clinical samples. **b** SERS intensity at 1334 cm^{-1} of the T region of the corresponding SERS ICA strips

B (N7), *Salmonella paratyphi* C (N8), *Yersinia enterocolitica* (N9), and *Staphylococcus aureus* (N10) positive but rotavirus negative samples were detected by the SERS ICA strips, only C line was observed from the strips and almost no SERS signals were recorded from the T line region, indicating that the SERS strip is highly specific to rotavirus.

Repeatability of SERS ICA strips

Figure 6a is the SERS spectrum of the T line region of 10 different test strips in the same batch detecting rotavirus standard samples with the same concentration. A good uniformity on the Raman spectra was observed from the T line region of these 10 strips and the relative standard deviation calculated from the SERS intensity of the main peak at 1334 cm^{-1} is less than 9%, exhibiting good reproducibility within the batch. Similar SERS spectra were also obtained from the T line region of 8 different batches of SERS ICA strips when detecting rotavirus standard samples with the same concentration (Fig. 6b). The relative standard deviation of the signal intensity of the main peak record from the T line region of these strips is 9.5%, exhibiting high repeatability between batches.

Table 2 Comparison of SERS ICA detection results from clinical samples with those of RT-qPCR and colloidal gold ICA

SERS ICA	RT-qPCR			Colloidal gold ICA		
	+	-	Sum	+	-	Sum
+	85	0	85	85	0	85
-	0	10	10	0	10	10
Sum	85	10	95	85	10	95

Clinical sample detection

The presence of rotavirus in 95 clinical samples was detected by SERS ICA assay, RT-qPCR, and colloidal gold ICA to determine the validity of the established technique. From Fig. 7a, obvious red T line and C line were observed from all SERS ICA strips loading with rotavirus-positive samples, while only red C line was observed from those loading with rotavirus-negative samples. The SERS signal at 1334 cm^{-1} of the T region of strips detecting rotavirus-positive samples is higher than 50,000 a.u., while the SERS signal is lower than the detection limit when negative sample was detected (Fig. 7b). Based on the SERS signal intensity of the main peak, a coincidence rate of 100% between SERS ICA assay and RT-qPCR as well as colloidal gold ICA was obtained (Table 2).

Comparison with other assays for diarrhea virus detection

A variety of methods have been developed for the detection of rotavirus, and their performance is shown in Table 3. The reported LOD for Au ICA and ELISA is $1 \times 10^3\text{ TCID}_{50}/0.1\text{ mL}$ and $1 \times 10^{2.5}\text{ TCID}_{50}/\text{mL}$, respectively [28, 29]. Due to the difference in the unit used, it is not suitable to compare them with developed SERS ICA. The weight of a rotavirus is approximately 10 fg; thus, the LOD for the SERS ICA can be approximated as 800 cfu/mL, which is much lower than that of LSPR, SERS, and PCBT [30–34]. In addition, the time consumed for the SERS ICA is much less than that of the other methods, except Au ICA.

However, it should be mentioned that the fabrication process and the detection procedure of the proposed method are complicated, which might limit their applications in high-

Table 3 Comparison of detection performance with other methods

Strategy	Samples	LOD	Time consumed	Reference
Au ICA	Fecal samples	1×10^3 TCID ₅₀ /0.1 mL	10 min	[28]
ELISA	Fecal samples	$1 \times 10^{2.5}$ TCID ₅₀ /mL	4 h	[29]
LSPR	Culture virus	1×10^3 PFU/mL	14 h	[30]
SERS	Culture virus	1×10^4 PFU/mL	30 min	[31]
PCBT	Culture virus	0.18×10^4 PFU/mL	20 h	[32]
RT-PCR	Fecal samples	1×10^3 copies/mL	2 h	[33]
PCR	Culture virus	1.95×10^{-4} pg/ μ L RNA	2 h	[34]
SERS ICA	Fecal samples	8 pg/mL	30 min	This work

throughput examination. Besides, the stability of the SERS tag is lower than the conventional Au colloidal solutions. In the future, the stability of SERS tags can be increased by using more uniform Au cores prepared by other methods.

Conclusions

In conclusion, a SERS ICA-based double-layer Raman molecule-labeled Au-core Ag-shell NP was successfully developed for the rapid, sensitive, and quantitative detection of rotavirus in the feces. The enhanced Raman signals obtained from the plasmonic effect of Au and Ag, double-layer Raman molecules, and the hot-spot effect between the Au core and Ag shell enable the ultra-sensitive and quantitative detection in less than 30 min. Favoring the rapid development and easy availability of handheld Raman spectrometers, the SERS ICA can be applied to the direct measurement of rotavirus in feces samples without complicated pretreatments.

Supplementary Information The online version contains supplementary material available at <https://doi.org/10.1007/s00604-020-04670-4>.

Authors' contributions Yuxue Zhang and Gang Wu designed and performed research, analyzed data, and wrote the paper; Jia-ta Wei and Yanlei Ding performed research and analyzed data; Yingming Wei revised the paper; Qiqi Liu and Hailan Chen designed research, analyzed data, revised, and proofread the paper.

Funding The study is financially supported by the National Major Science and Technology Projects of China [2018ZX10711001-003-003], the National Natural Science Foundation of China [21763004], and the Nanning Excellent Young Scientist Program [RC20190102].

Data availability The datasets generated during and/or analyzed during the current study are available from the corresponding author on reasonable request.

Compliance with ethical standards **Informed consent was obtained from all individual participants involved in the study.**

Conflict of interest The authors declare that they have no conflict of interest.

References

- Diez-Valcarce M, Lopez MR, Lopez B, Morales O, Sagastume M, Cadena L, Kaydos-Daniels S, Jarquin C, McCracken JP, Bryan JP, Vinjé J (2019) Prevalence and genetic diversity of viral gastroenteritis viruses in children younger than 5 years of age in Guatemala, 2014–2015. *J Clin Virol* 114:6–11. <https://doi.org/10.1016/j.jcv.2019.03.006>
- Madhi SA, Cunliffe NA, Steele D, Witte D, Kirsten M, Louw C, Ngwira B, Victor JC, Gillard PH, Chevart BB (2016) Effect of human rotavirus vaccine on severe diarrhea in African infants. *Malawi Med J* 28(4):289–298. <https://doi.org/10.1056/nejmoa0904797>
- Rheingans R, Anderson JDt, Bagamian KH, Pecenka CJ (2018) Effects of geographic and economic heterogeneity on rotavirus diarrhea burden and vaccination impact and cost-effectiveness in the Lao People's Democratic Republic. *Vaccine* 36(51):7868–7877. <https://doi.org/10.1016/j.vaccine.2018.02.009>
- Vidal A, Martín-Valls GE, Tello M, Mateu E, Martín M, Darwich L (2019) Prevalence of enteric pathogens in diarrheic and non-diarrheic samples from pig farms with neonatal diarrhea in the north east of Spain. *Vet Microbiol* 237:108419. <https://doi.org/10.1016/j.vetmic.2019.108419>
- Weitkamp JH, Kallewaard N, Kuschara K, Feigelstock D, Feng N, Greenberg HB, Crowe JE Jr (2003) Generation of recombinant human monoclonal antibodies to rotavirus from single antigen-specific B cells selected with fluorescent virus-like particles. *J Immunol Methods* 275(1):223–237. [https://doi.org/10.1016/S0022-1759\(03\)00013-9](https://doi.org/10.1016/S0022-1759(03)00013-9)
- Kawai K, O'Brien MA, Goveia MG, Mast TC, El Khoury AC (2012) Burden of rotavirus gastroenteritis and distribution of rotavirus strains in Asia: a systematic review. *Vaccine* 30(7):1244–1254. <https://doi.org/10.1016/j.vaccine.2011.12.092>
- Elschner M, Prudlo J, Hotzel H, Otto P, Sachse K (2010) Nested reverse transcriptase-polymerase chain reaction for the detection of group A rotaviruses. *J Vet Med B Infect Dis Vet Public Health* 49(2):77–81. <https://doi.org/10.1046/j.1439-0450.2002.00510.x>
- Choe JY, Kim JW, Kwon HH, Hong HL, Jung CY, Jeon CH, Park EJ, Kim SK (2020) Diagnostic performance of immunochromatography assay for rapid detection of IgM and IgG in coronavirus disease 2019. *J Med Virol* 92:2567–2572. <https://doi.org/10.1002/jmv.26060>
- Greenberg HB, McAuliffe V, Valdesuso J, Wyatt RG, Singh NH (1983) Serological analysis of the subgroup protein of rotavirus,

- using monoclonal antibodies. *Infect Immun* 39(1):91–99. <https://doi.org/10.1128/IAI.39.1.91-99.1983>
10. Yu J, Lai S, Geng Q, Ye C, Zhang Z, Zheng Y, Wang L, Duan Z, Zhang J, Wu S, Parashar U, Yang W, Liao Q, Li Z (2019) Prevalence of rotavirus and rapid changes in circulating rotavirus strains among children with acute diarrhea in China, 2009–2015. *J Inf Secur* 78(1):66–74. <https://doi.org/10.1016/j.jinf.2018.07.004>
 11. Huang D, Lin B, Song Y, Guan Z, Cheng J, Zhu Z, Yang C (2019) Staining traditional colloidal gold test strips with Pt nanoshell enables quantitative point-of-care testing with simple and portable pressure meter readout. *ACS Appl Mater Interfaces* 11(2):1800–1806. <https://doi.org/10.1021/acsami.8b15562>
 12. Mukunzi D, Suryoprabowo S, Song S, Liu L, Kuang H (2018) Development of an indirect enzyme-linked immunosorbent assay and lateral-flow test strips for pefloxacin and its analogues in chicken muscle samples. *Food Agric Immunol* 29(1):484–497. <https://doi.org/10.1080/09540105.2017.1406460>
 13. Zuo J-Y, Jiao Y-J, Zhu J, Ding S-N (2018) Rapid detection of severe fever with thrombocytopenia syndrome virus via colloidal gold immunochromatography assay. *ACS Omega* 3(11):15399–15406. <https://doi.org/10.1021/acsomega.8b02366>
 14. Urusov AE, Zherdev AV, Dzantiev BB (2019) Towards lateral flow quantitative assays: detection approaches. *Biosensors (Basel)* 9(3). <https://doi.org/10.3390/bios9030089>
 15. Kawai K, O'Brien MA, Goveia MG, Mast TC, Khoury ACE (2012) Burden of rotavirus gastroenteritis and distribution of rotavirus strains in Asia: a systematic review. *Vaccine* 30(7):1244–1254. <https://doi.org/10.1016/j.vaccine.2011.12.092>
 16. Yan W, Yang L, Zhuang H, Wu H, Zhang J (2016) Engineered “hot” core-shell nanostructures for patterned detection of chloramphenicol. *Biosens Bioelectron* 78:67–72. <https://doi.org/10.1016/j.bios.2015.11.011>
 17. Tivanov MS, Kolesov EA, Korolik OV, Saad AM, Kovalchuk NG, Komissarov IV, Labunov VA, Opielak M, Zukowski P, Koltunowicz TN (2018) Raman spectra of graphene synthesized by chemical vapor deposition from decane. *J Appl Spectrosc* 84(6):979–985. <https://doi.org/10.1007/s10812-018-0574-z>
 18. Li X, Yang T, Song Y, Zhu J, Wang D, Li W (2019) Surface-enhanced Raman spectroscopy (SERS)-based immunochromatographic assay (ICA) for the simultaneous detection of two pyrethroid pesticides. *Sensor Actuat B-Chem* 283:230–238. <https://doi.org/10.1016/j.snb.2018.11.112>
 19. Deng D, Yang H, Liu C, Zhao K, Li J, Deng A (2019) Ultrasensitive detection of diclofenac in water samples by a novel surface-enhanced Raman scattering (SERS)-based immunochromatographic assay using AgMBA@SiO₂-Ab as immunoprobe. *Sensor Actuat B-Chem* 283:563–570. <https://doi.org/10.1016/j.snb.2018.12.076>
 20. Wang X, Choi N, Cheng Z, Ko J, Chen L, Choo J (2017) Simultaneous detection of dual nucleic acids using a SERS-based lateral flow assay biosensor. *Anal Chem* 89(2):1163–1169. <https://doi.org/10.1021/acs.analchem.6b03536>
 21. Hwang J, Lee S, Choo J (2016) Application of a SERS-based lateral flow immunoassay strip for the rapid and sensitive detection of staphylococcal enterotoxin B. *Nanoscale* 8(22):11418–11425. <https://doi.org/10.1039/C5NR07243C>
 22. Blanco-Covián L, Montes-García V, Girard A, Fernández-Abedul MT, Pérez-Juste J, Pastoriza-Santos I, Faulds K, Graham D, Blanco-López MC (2017) Au@Ag SERRS tags coupled to a lateral flow immunoassay for the sensitive detection of pneumolysin. *Nanoscale* 9(5):2051–2058. <https://doi.org/10.1039/c6nr08432j>
 23. Gao X, Zheng P, Kasani S, Wu S, Yang F, Lewis S, Nayeem S, Engler-Chiurazzi EB, Wigginton JG, Simpkins JW, Wu N (2017) Paper-based surface-enhanced Raman scattering lateral flow strip for detection of neuron-specific enolase in blood plasma. *Anal Chem* 89(18):10104–10110. <https://doi.org/10.1021/acs.analchem.7b03015>
 24. Zhang L, Huang Y, Wang J, Rong Y, Lai W, Zhang J, Chen T (2015) Hierarchical flowerlike gold nanoparticles labeled immunochromatography test strip for highly sensitive detection of *Escherichia coli* O157:H7. *Langmuir* 31(19):5537–5544. <https://doi.org/10.1021/acs.langmuir.5b00592>
 25. Jia X, Wang C, Rong Z, Li J, Wang K, Qie Z, Xiao R, Wang S (2018) Dual dye-loaded Au@Ag coupled to a lateral flow immunoassay for the accurate and sensitive detection of *Mycoplasma pneumoniae* infection. *RSC Adv* 8(38):21243–21251. <https://doi.org/10.1039/C8RA03323D>
 26. Zhang C, Liang X, You T, Yang N, Gao Y, Yin P (2017) An ultrasensitive “turn-off” SERS sensor for quantitatively detecting heparin based on 4-mercaptobenzoic acid functionalized gold nanoparticles. *Anal Methods-UK* 9(17):2517–2522. <https://doi.org/10.1039/C7AY00494J>
 27. Fang W, Zhang X, Chen Y, Wan L, Huang W, Shen A, Hu J (2015) Portable SERS-enabled micropipettes for microarea sampling and reliably quantitative detection of surface organic residues. *Anal Chem* 87(18):9217–9224. <https://doi.org/10.1021/acs.analchem.5b01635>
 28. Development of a colloidal gold immunochromatographic strip assay for rapid detection of bovine rotavirus. *Viral Immunol* 2019, 32(9):393–401. <https://doi.org/10.1089/vim.2019.0071>
 29. (2017) Development and validation of monoclonal antibody-based antigen capture ELISA for detection of group A porcine rotavirus. *Viral Immunol* 30(4):264–270. <https://doi.org/10.1089/vim.2016.0154>
 30. Rippa M, Castagna R, Brandi S, Fusco G, Monini M, Chen D, Zhou J, Zyss J, Petti L (2020) Octupolar plasmonic nanosensor based on ordered arrays of triangular Au nanopillars for selective rotavirus detection. *ACS Applied Nano Materials* 3(5):4837–4844. <https://doi.org/10.1021/acsnano.0c00872>
 31. Driskell JD, Zhu Y, Kirkwood CD, Zhao Y, Dluhy RA, Tripp RA (2010) Rapid and sensitive detection of rotavirus molecular signatures using surface enhanced Raman spectroscopy. *PLoS One* 5(4):e10222. <https://doi.org/10.1371/journal.pone.0010222>
 32. Pineda MF, Chan LL, Kuhlenschmidt T, Choi CJ, Kuhlenschmidt M, Cunningham BT (2009) Rapid specific and label-free detection of porcine rotavirus using photonic crystal biosensors. *IEEE Sensors J* 9(4):470–477. <https://doi.org/10.1109/JSEN.2009.2014427>
 33. Anaya-Molina Y, De La Cruz Hernández SI, Andrés-Dionicio AE, Terán-Vega HL, Méndez-Pérez H, Castro-Escarpullí G, García-Lozano H (2018) A one-step real-time RT-PCR helps to identify mixed rotavirus infections in Mexico. *Diagn Microbiol Infect Dis* 92(4):288–293. <https://doi.org/10.1016/j.diagmicrobio.2018.06.023>
 34. Joshi MS, Deore SG, Walimbe AM, Ranshing SS, Chitambar SD (2019) Evaluation of different genomic regions of rotavirus A for development of real time PCR. *J Virol Methods* 266:65–71. <https://doi.org/10.1016/j.jviromet.2019.01.017>

Publisher's note Springer Nature remains neutral with regard to jurisdictional claims in published maps and institutional affiliations.